Article

Immunity guided identification of threonyl-tRNA synthetase as the molecular target of obafluorin, a beta-lactone antibiotic

Thomas A Scott, Sibyl F. D. Batey, Patrick Wiencek, Govind Chandra, Silke Alt, Christopher S. Francklyn, and Barrie Wilkinson

ACS Chem. Biol., **Just Accepted Manuscript** • DOI: 10.1021/acschembio.9b00590 • Publication Date (Web): 01 Nov 2019

Just Accepted

is published by the American Chemical Society. 1155 Sixteenth Street N.W., Washington, DC 20036

Immunity guided identification of threonyl-tRNA synthetase as the molecular target of obafluorin, a *β*-lactone antibiotic

Thomas A. Scott,[ac†] Sibyl F. D. Batey,[a†] Patrick Wiencek,[b] Govind Chandra,[a] Silke Alt,[a] Christopher S. Franklyn[b*] and Barrie Wilkinson[a*]

[a] *Department of Molecular Microbiology, John Innes Centre, Norwich Research Park, Norwich NR4 7UH, UK*

[b] *Department of Biochemistry, College of Medicine, University of Vermont, Burlington, VT 05405, USA*

[c] *Current address: Institute of Microbiology, Eidgenössische Technische Hochschule (ETH) Zürich, Vladimir-Prelog-Weg 4, 8093 Zürich, Switzerland*

† These authors contributed equally to this work.

*Email: barrie.wilkinson@jic.ac.uk

Abstract

To meet the ever-growing demands of antibiotic discovery, new chemical matter and antibiotic targets are urgently needed. Many potent natural product antibiotics which were previously discarded can also provide lead molecules and drug targets. One such example is the structurally unique *β*-lactone obafluorin, produced by *Pseudomonas fluorescens* ATCC 39502. Obafluorin is active against both Gram-positive and -negative pathogens, however the biological target was unknown. We now report that obafluorin targets threonyl-tRNA synthetase and we identify a homologue, ObaO, which confers immunity to the obafluorin producer. Disruption of *obaO* in *P. fluorescens* ATCC 39502 results in obafluorin sensitivity, whereas expression in sensitive *E. coli* strains confers resistance. Enzyme assays demonstrate that *E. coli* threonyl-tRNA synthetase is fully inhibited by obafluorin, whereas ObaO is only partly susceptible, exhibiting a very unusual partial inhibition mechanism. Altogether, our data highlight the utility of an immunity-guided approach for the identification of an antibiotic target *de novo* and will ultimately enable the generation of improved obafluorin variants.

Introduction

Natural products, especially those produced by microorganisms, account for approximately 80% of all antibiotics in clinical use.[1] Moreover, numerous other natural products have been identified with potent antibacterial activity but have failed to progress into clinical use, or even investigation, due to confounding activities such as off target effects, poor bioavailability, or a lack of broad-spectrum activity. Given recent predictions that infectious disease will become the biggest killer of humans by 2050 due to the alarming increase in antimicrobial resistance,[2] reevaluation of these previously discarded natural products is timely. By focusing on structurally unique molecules we hypothesize that new targets and modes of action might be uncovered and provide an opportunity to avoid cross resistance with existing clinical classes. One such molecule is the *β*-lactone antibiotic obafluorin (**1**).

β-Lactone rings occur infrequently in Nature but are constituents of several different natural product classes.[3] Structurally similar to *β*-lactam rings, they are effective electrophiles able to form covalent linkages with nucleophilic residues of target proteins[4] and possess significant therapeutic value as hydrolase inhibitors.[5] Prominent examples include the hybrid polyketide-non-ribosomal peptide (PK-NRP) Salinosporamide A (marizomib), which is a potent 20S proteasome inhibitor that is currently in Phase III clinical trials as a treatment for glioblastoma,[6] and tetrahydolipstatin (orlistat), a semi-synthetic derivative of the PK-NRP lipstatin approved by the US Food and Drug Administration for the treatment of obesity due to its powerful lipase inhibitory activity.[7] Further validated targets of *β*-lactone inhibitors include serine hydrolase and polyketide synthase enzymes associated with mycolic acid biosynthesis, inhibition of which is lethal for *Mycobacterium tuberculosis*,[8] as well as esterases, cutinases, homoserine transacetylase, cathespin A, ClpP and *N*-acylethanolamine acid amidase.[9, 10]

Due to their therapeutic potential, much effort has been put into elucidating the genetic and biochemical basis for *β*-lactone ring formation during natural product biosynthesis.[11] Recent work in our lab[12] and by others[13] characterized the biosynthetic pathway to the *β*-lactone antibiotic **1** from *Pseudomonas fluorescens* ATCC 39502. **1** is assembled by ObaI, a bimodular non-ribosomal peptide synthetase which catalyzes amide bond formation between 2,3-dihydroxybenzoic acid (**2**), and the nonproteinogenic amino acid (2*S*,3*R*)-2-amino-3-hydroxy-4-(4-nitrophenyl)butanoate

(**3**), the product of a rare L-threonine transaldolase (Figure 1).[12] Critically, it is this unusual *β*-hydroxy-*α*-amino acid precursor that comprises the functional groups which give rise to the *β*-lactone ring of **1**, following cyclization catalyzed by a rare type I thioesterase domain present in ObaI, which possesses a noncanonical active site Cys residue.

Despite undergoing facile hydrolysis and ring opening in the presence of nucleophiles, **1** exhibits potent antibacterial activity against a range of Gram-positive bacteria and is also active against Gram-negative bacteria including *E. coli* and various *Pseudomonas aeruginosa* strains (Table 1 and Supplementary Figure 1).[14, 15] When dosed systemically, it protects mice challenged with *Streptococcus pyogenes* (ED_{50} = 50 mg kg^{-1}) and is also reported to cause an unusual cell-elongation phenotype in *E. coli* cells exposed to sub-lethal doses. These various observations suggest that **1** acts in a specific manner rather than as a general acylating agent, yet, despite this unusual activity profile, the molecular target for **1** remained obscure. Given the urgent need for new antibacterial targets for antibiotic development, we turned our attention to identifying the molecular target of **1**.

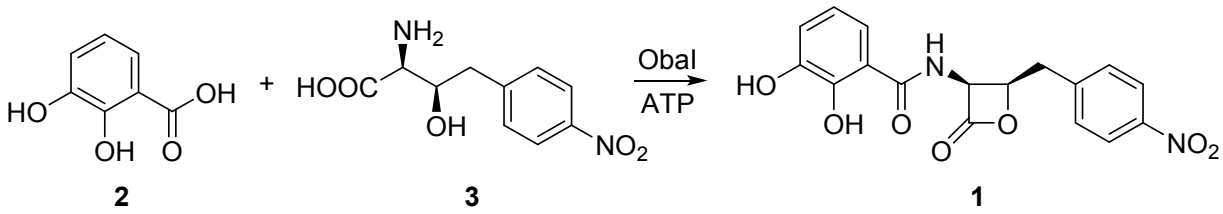

2 **3** **1**

Figure 1 Biosynthesis of obafluorin (**1**) in *P. fluorescens* ATCC 39502 from 2,3-dihydroxybenzoic acid (**2**) and (2*S*,3*R*)-2-amino-3-hydroxy-4-(4-nitrophenyl)butanoate (**3**).

RESULTS AND DISCUSSION

Bioinformatic analysis identifies a putative 1 **immunity gene.** We set out to identify the target of **1** using an immunity-guided approach, combining genetic analyses with chemical complementation, bioassays, and *in vitro* enzyme assays. We began our investigation by examining the genomic neighborhood surrounding the *oba* biosynthetic gene cluster (BGC) (MiBIG accession: BGC0001437; GenBank accession: KX931446.2) in search of immunity gene candidates. Genes encoding immunity determinants commonly co-occur with the biosynthetic loci required for the production of natural product antibiotics,[16] a phenomenon that has inspired recent genome-mining efforts to identify novel scaffolds with known targets.[17-19] Comparative genomic analysis of the *oba* BGC characterized in *P. fluorescens* ATCC 39502 with other putative **1** BGCs present in the genomes of two *P. fluorescens* soil isolates, several *Burkholderia* species and *Chitiniphilus shinanonensis* DSM 23277 (Supplementary Table 1) allowed the identification of a minimal set of genes conserved across all clusters (Figure 2). In addition to those previously ascribed biosynthetic or regulatory functions,[12] only one additional gene, encoding a putative threonyl-tRNA synthetase (ThrRS), was present in all putative **1** BGCs; we have named this gene *obaO* (GenBank accession: KX931446.2).

Aminoacyl-tRNA synthetases (aaRSs) play an essential role in protein synthesis, specifically activating and loading amino acids onto their cognate tRNAs.[20] Although ubiquitous, divergence in aaRS sequence structure has led to the evolution of natural product (NP) antibiotics that selectively target those of competing organisms.[21, 22] aaRS-targeting NPs have been applied in both crop protection and clinical use, with the LeuRS inhibitor Agrocin TM84 used to treat crown gall disease[23] and the IleRS inhibitor mupirocin used topically in humans to treat skin infections.[24] ThrRS is targeted by the polyketide NP borrelidin, which acts by simultaneously occupying the three catalytic subsites, along with a non-catalytic fourth subsite.[25, 26] In several instances, an immunity isoform of the target aaRS is encoded within the NP BGC as an addition to the primary housekeeping copy encoded elsewhere in the genome of the producing-organism.[27-29] Indeed, the putative *oba* BGC-associated ThrRS homologues all represent second copies in their respective genomes and, likewise, an additional copy of ThrRS is only observed in the presence of the *oba* BGC amongst these genera.

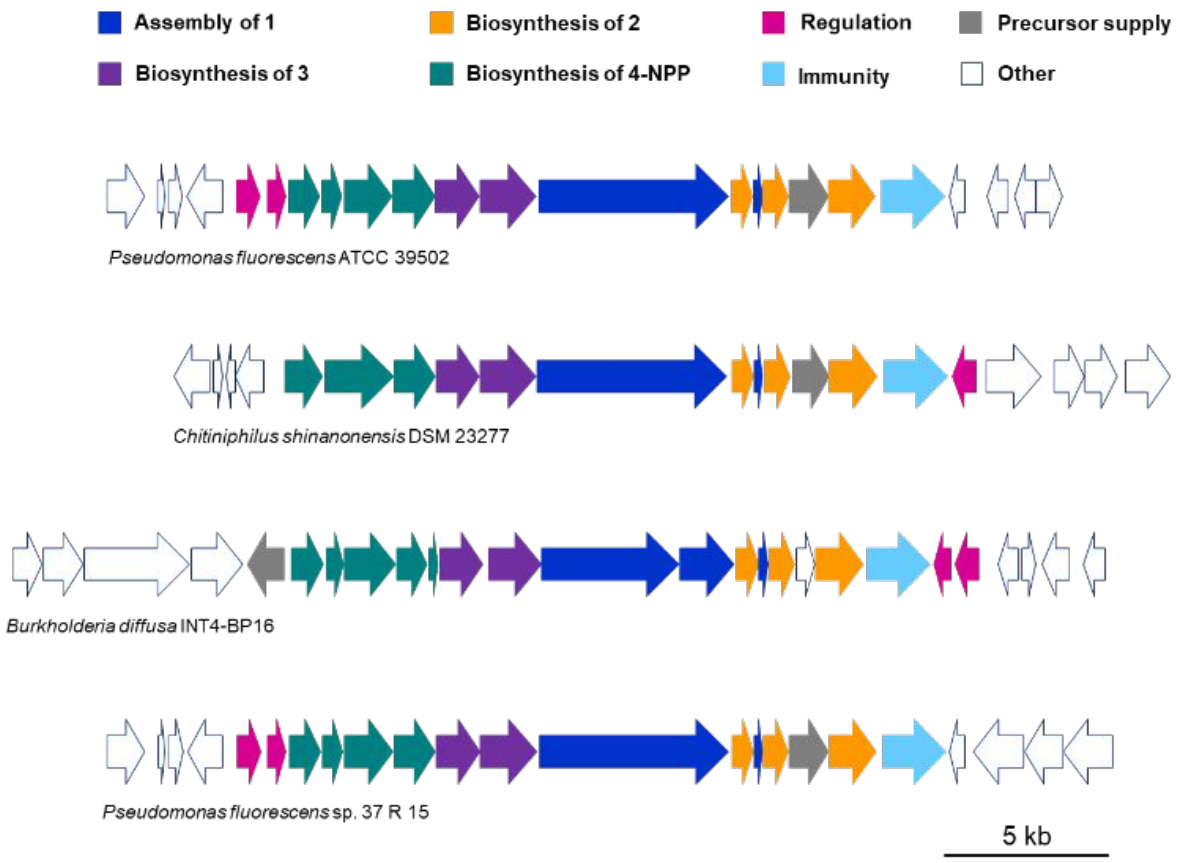

Figure 2 Comparative analysis of obafluorin (**1**) biosynthetic gene clusters. Genes are color-coded according to their function, with putative immunity colored in light blue. 4-NPP = 4-Nitrophenylpyruvate, an intermediate in the biosynthesis of (2*S*,3*R*)-2-amino-3-hydroxy-4-(4-nitrophenyl)butanoate (**3**).

***obaO* confers immunity to 1 in the native producer.** To confirm the ability of ObaO to confer **1** immunity in the native producer, we attempted *obaO* inactivation experiments using the pTS1 suicide vector generated previously[12] to perform knockouts in biosynthetic *oba* genes. However, following double crossover and counter-selection, we observed that resulting colonies were always exclusively wild-type (WT), consistent with a selection pressure against losing the immunity determinant when the *oba* BGC is functional.

To circumvent this issue, we deleted *obaO* in a Δ*obaL* background in which **1** production is abolished but can be rescued by exogenous supplementation with **2**. In the absence of exogenous **2** the growing strains accumulate increased levels of the shunt metabolites 4-nitrophenylethanol and 4-nitrophenylacetate, which is indicative of an otherwise functional biosynthetic pathway.[12] We were successful in generating the Δ*obaL*Δ*obaO* strain and resulting mutants were verified by PCR amplification

across the newly deleted region, with subsequent sequencing of the amplicon. When the Δ*obaL*Δ*obaO* strain was grown in production medium supplemented with **2**, growth was strongly inhibited, in contrast to cultures of WT and Δ*obaL* supplemented with **2**, and un-supplemented controls (Figure 3). The Δ*obaL*Δ*obaO* strain was complemented genetically by ectopic expression of *obaO* using the pJH10TS vector described previously,[12] which restored WT-like growth and **1** production when the strain was grown in **2**-supplemented production medium (Figure 3). Taken together, these observations are consistent with a role for ObaO in conferring immunity to **1** in the native producer, *P. fluorescens* ATCC 39502.

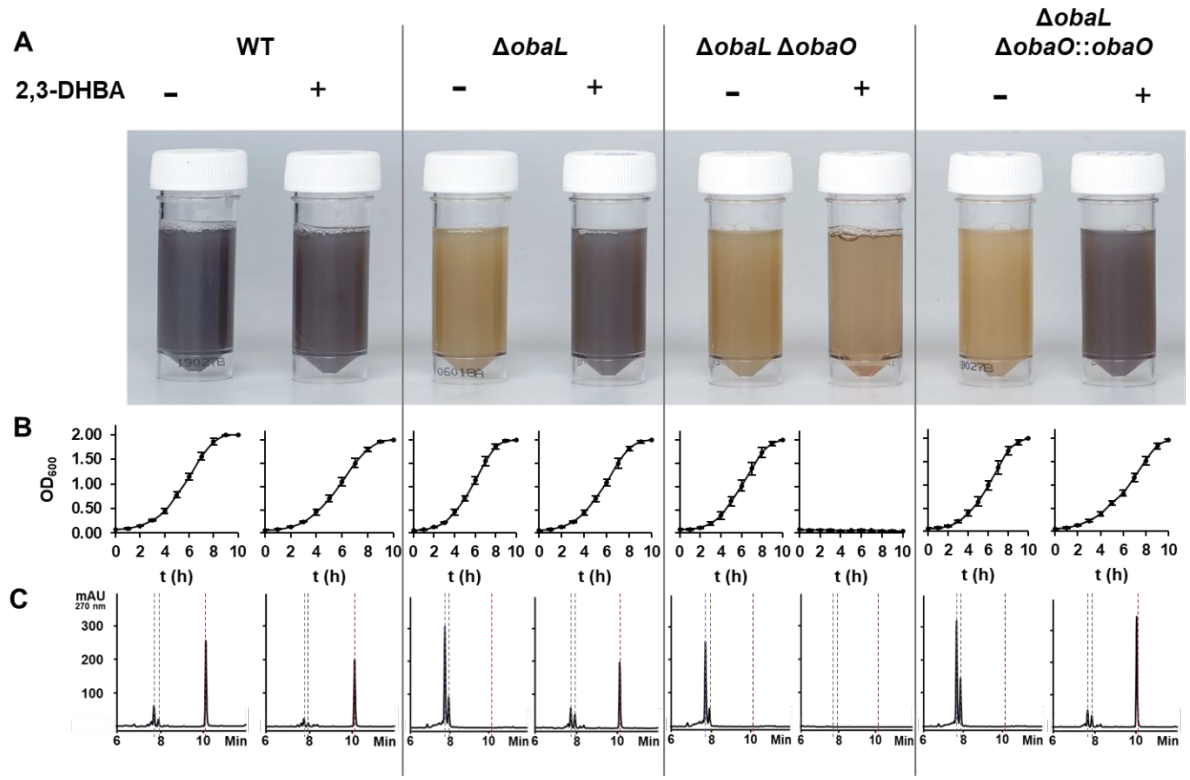

Figure 3 ObaO is the immunity determinant for 1 in *P. fluorescens* 39502. WT, Δ*obaL*, Δ*obaL*Δ*obaO* and Δ*obaL*Δ*obaO::obaO* strains were grown ± 2,3-dihydroxybenzoic acid (2,3-DHBA, **2**) (0.2 mM). As shown previously,[12] **2** restores obafluorin (**1**) production for Δ*obaL*, whereas the addition of **2** to Δ*obaL*Δ*obaO* abolishes growth. **a**) Aliquots of each strain after 14 h growth, with the purple coloration being indicative of **1** production. **b**) Log phase growth curves, showing complete absence of growth for Δ*obaL*Δ*obaO* + **2**. Each data point is the average of three biological repeats and bars show the standard error. **c**) Representative HPLC chromatograms at 270 nm for each condition at 14 h; **1** elutes at 10.1 min (red dashed line) and the shunt metabolites 4-nitrophenylethanol (blue dashed line) and 4-nitrophenylacetate (green dashed line) elute at 7.7 min and 7.9 min respectively.

***obaO* confers high-level resistance to 1-sensitive *E. coli* strains.** To further validate our hypothesis, we introduced the *obaO* gene into **1**-sensitive bacterial strains to investigate its ability to confer resistance to those strains when challenged with **1**. Given that *E. coli* was previously identified as being sensitive to **1**,[14] we tested the reference strain *E. coli* ATCC 25922, and *E. coli* NR698 which has increased permeability to antibiotics due to compromised outer-membrane lipopolysaccharide assembly.[30] Off-target reactions of **1** with culture medium components precluded the use of microbroth assays, so we turned to disc-diffusion based approaches. We found that **1** binds to paper discs, as reported previously,[31] so we instead employed a spot-on-lawn approach by directly applying a solution of **1** dissolved in acetonitrile to the surface of agar bioassay plates. Using this method, **1** was shown to have a minimum inhibitory concentration (MIC) of 256 μg mL^{-1} for *E. coli* 25922, and 4 μg mL^{-1} for *E. coli* NR698 (Figure 4, Table 1 and Supplementary Figure 1). However, when *obaO* was expressed ectopically in both strains using the pJH10TS vector, both became resistant to **1** up to the highest concentration tested of 2000 μg mL^{-1}. This represents increases in the MIC of **1** of at least 8- and 250-fold for *E. coli* ATCC 25922 and *E. coli* NR698, respectively, relative to empty vector controls. Therefore, *obaO* confers transferable high-level resistance to **1**.

To determine whether simple overexpression of an additional copy of ThrRS is sufficient to provide resistance to **1**, we turned our attention to the primary housekeeping versions of ThrRS present in *P. fluorescens* ATCC 39502 (PfThrRS) and *E. coli* (EcThrRS; GenBank accession: WP_001144202.1). The Δ*obaL*Δ*obaO* strain was complemented by ectopic expression of the genes encoding either PfThrRS or EcThrRS (amplified from *E. coli* BL21 (DE3)) using the pJH10TS vector[12] and was then grown in production medium supplemented with **2** to activate **1** biosynthesis. We observed that culture growth plateaued after 5 h and that the production of **1** was not restored in both cases (Figure 5, panel a). A similar phenotype was observed in the IleRS mupirocin immunity gene knock out and attributed to the stringent response, resulting from amino acid starvation.[32] Thus, we hypothesize that **1** is initially produced in growing cells but reaches localized levels that inhibit the elevated levels of ThrRS leading to accumulation of uncharged $tRNA^{Thr}$ and induction of the stringent response. This results in transcriptional shutdown of non-essential genes and is consistent with the observed growth inhibition, and the lack of accumulated shunt metabolites and **1**

(Figure 5, panel a). In contrast, the un-supplemented control suffers minimal growth defects and retains the ability to accumulate shunt metabolites. Similarly, we found that when *E. coli* bioassay strains expressing either an additional copy of their native EcThrRS or PfThrRS were challenged with **1**, there was only a modest increase in **1**-resistance for *E. coli* NR698, with a **1** MIC of 16 μg mL^{-1} (2-fold increase versus control). The MIC of **1** against *E. coli* 25922 was unchanged at 256 μg mL^{-1} (Figure 5, panel b and Table 1). This suggested that ObaO functions as the primary **1** resistance determinant.

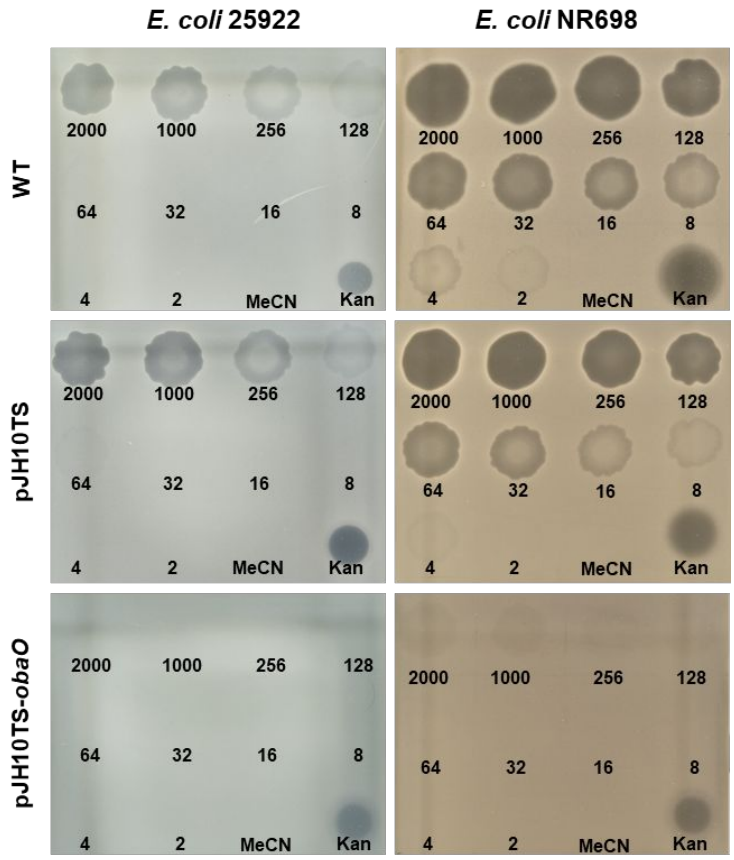

Figure 4 ObaO confers transferable immunity to obafluorin (**1**)-sensitive *E. coli* strains. **1** spot-on-lawn assays with reference strain *E. coli* 25922 and permeable strain *E. coli* NR698, with zones of clearing indicating growth inhibition. Numbers indicate **1** concentrations (in μg mL^{-1}), with MeCN as a negative control and kanamycin (50 μg mL^{-1}) as a positive control. ObaO confers resistance to >2000 μg mL^{-1} **1**, in contrast to the WT strains and empty vector controls. Images are representative of three biological repeats for each strain.

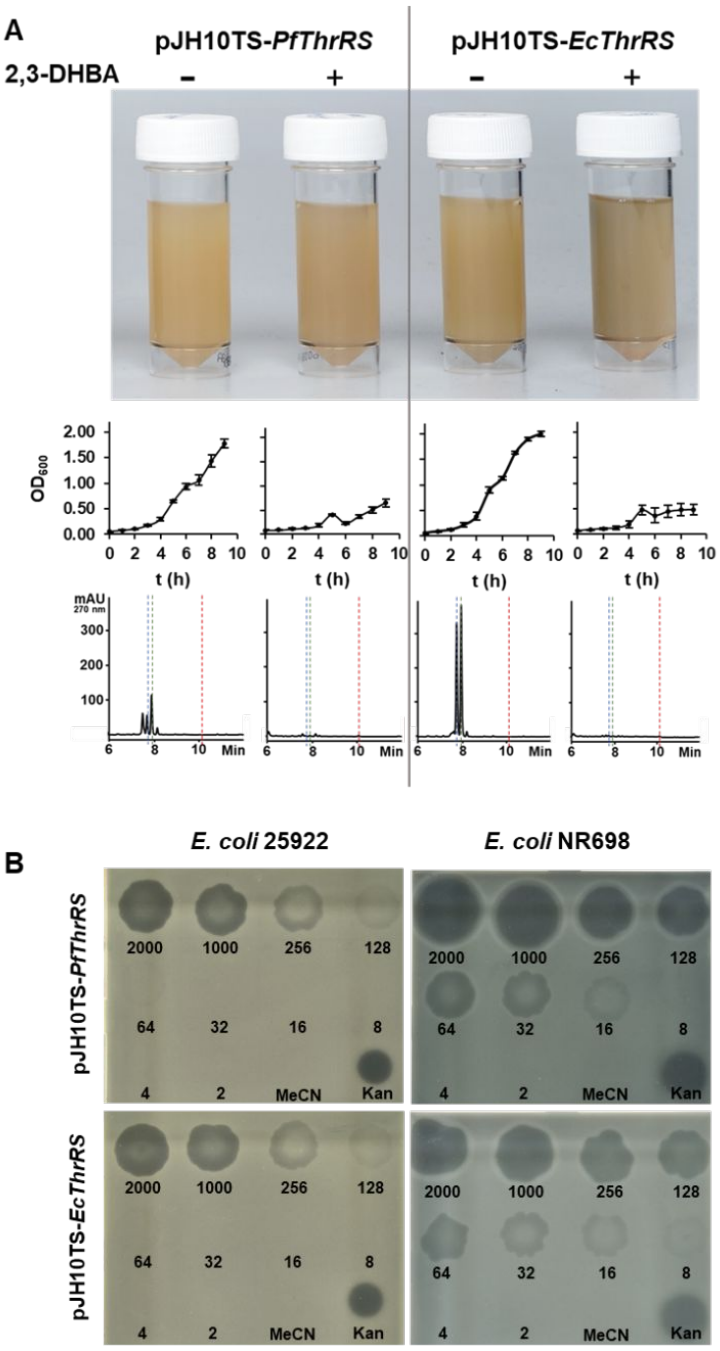

Figure 5 PfThrRS and EcThrRS do not confer immunity to obafluorin (**1**)**. a**) Complementation of *P. fluorescens* Δ*obaL*Δ*obaO* with ThrRS genes. Δ*obaL*Δ*obaO* was complemented with *PfThrRS* or *EcThrRS* in pJH10TS and grown ± 2,3-dihydroxybenzoic acid (2,3-DHBA, **2**) (0.2 mM). In contrast to *obaO* (Figure 3) growth plateaued after ~5 h for *PfThrRS* and *EcThrRS* strains fed with **2**, and **1** production was not restored. Aliquots of cultures after 14 h growth, log phase growth curves and representative HPLC chromatograms are shown, analogous to Figure 3. Each growth curve data point is the average of three biological repeats, with bars showing the standard error and HPLC analysis was carried out on every biological repeat. **1** is initially produced in growing cells but reaches localized levels that inhibit the elevated levels of ThrRS, leading to accumulation of uncharged $tRNA^{Thr}$ and induction of the stringent response. This is consistent with the observed growth inhibition and the lack

of accumulated shunt metabolites and **1**. **b**) **1** spot-on-lawn assays as in Figure 4, with reference strain *E. coli* 25922 and permeable strain *E. coli* NR698 overexpressing either PfThrRS or an additional copy of EcThrRS: in contrast to ObaO, there is no difference in the MIC value for strain *E. coli* 25922 and a modest 2-fold increase in MIC for strain *E. coli* NR698. Images are representative of three biological repeats for each strain.

Strain	1 MIC (μg mL^{-1})
B. subtilis	4
MRSA	2
E. coli ATCC 25922	256
E. coli ATCC 25922 pJH10TS	256
E. coli ATCC 25922 pJH10TS-*obaO*	>2000
E. coli ATCC 25922 pJH10TS-*EcThrRS*	256
E. coli ATCC 25922 pJH10TS-*PfThrRS*	256
E. coli NR698	4
E. coli NR698 pJH10TS	8
E. coli NR698 pJH10TS-*obaO*	>2000
E. coli NR698 pJH10TS- *EcThrRS*	16
E. coli NR698 pJH10TS- *PfThrRS*	16

Table 1. Obafluorin (**1**) is active against both Gram-positive and Gram-negative bacteria. **1** MICs were determined by the spot-on-lawn method, as shown in Figures 4, Figure 5 and Supplementary Figure 1. Experiments were performed in triplicate for each strain. Further details on each strain can be found in Supplementary Table 2.

1 **is potent inhibitor of EcThrRS and a partial inhibitor of ObaO.** To confirm that **1** is a *bona fide* inhibitor of ThrRS, we examined the formation of Thr-tRNA^{Thr} by EcThrRS in the presence of 0–5 μM **1**. The rate of aminoacylation of tRNA decreased progressively over this concentration range, with complete inhibition occurring around 1 μM (Figure 6, panel a). Fitting of the data to a dose response equation returned an IC_{50} of 92 $\pm$ 21 nM, confirming that **1** is a potent inhibitor of EcThrRS (Figure 6, panel c). Aminoacylation assays with ObaO indicated that, in the absence of **1**, ObaO exhibits activity comparable to EcThrRS. When ObaO was challenged with increasing concentrations of **1**, aminoacylation was initially decreased but not completely inhibited at the highest concentrations of **1** (Figure 6, panel b). In order to fit the data

and derive an IC_{50}, a modified dose response equation was employed that includes a term denoting residual enzyme activity at saturating inhibitor concentrations.[33] Fitting the data to this equation gave an IC_{50} of 50 ± 25 nM and a fractional residual activity of 0.35 ± 0.07 (Figure 6, panel d), signifying a partial inhibition mechanism. This is a rarely reported phenomenon, whereby the activity of an enzyme cannot be driven to zero, even at the highest concentrations of inhibitor. It is often attributed to experimental artefacts, such as limited compound solubility at high concentrations,[33]

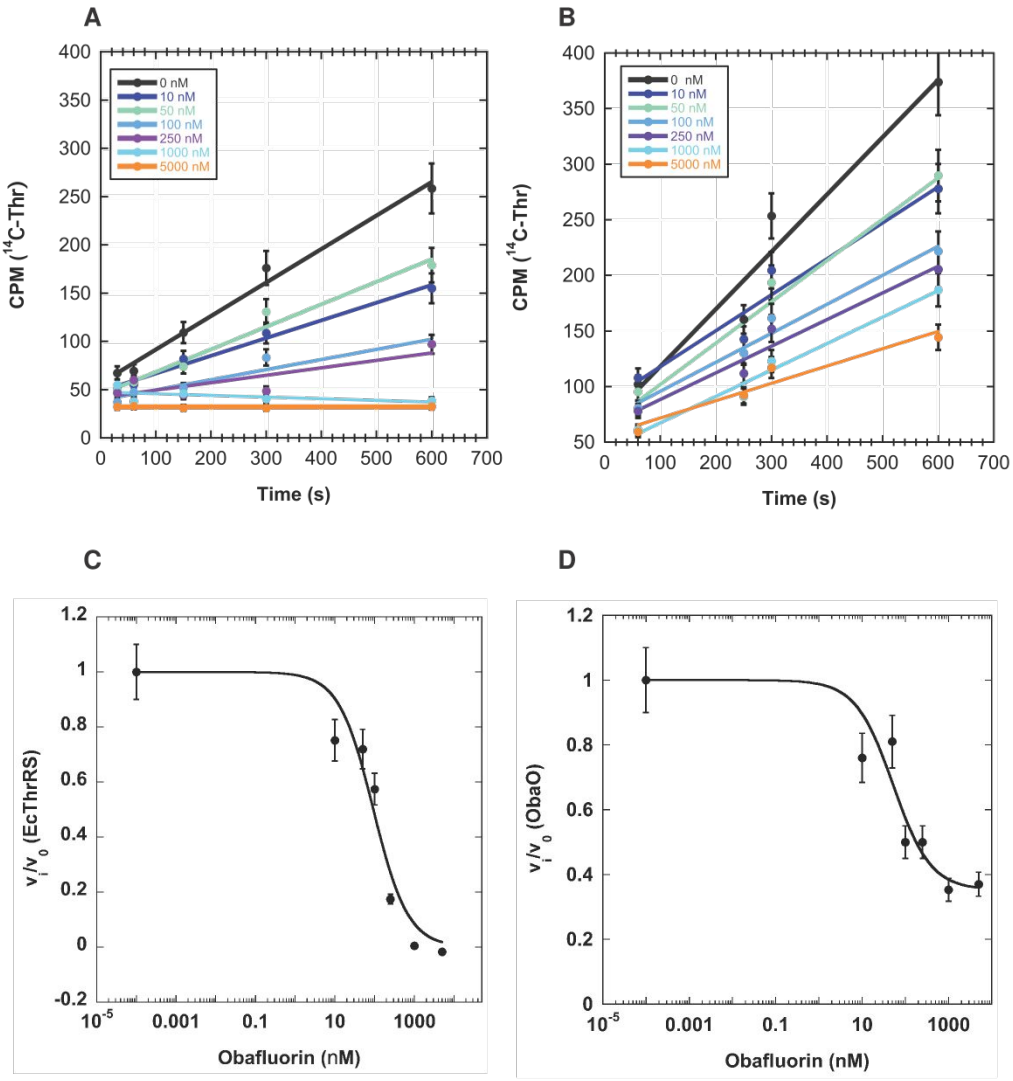

Figure 6 Complete and partial Inhibition of EcThrRS and ObaO, respectively, by obafluorin (**1**). Progress curves for EcThrRS (**a**) and ObaO (**b**) in the presence of varying (0–5 μM) concentrations of **1**. Enzyme (10 nM) and varying concentrations of **1** were pre-incubated for 30 min prior to adding to a reaction containing saturating substrates. Reactions (n = 3) included enzyme at 10 nM and saturating concentration of tRNA, threonine, and ATP. The progress curves were fit to a linear equation to derive initial rates. Error bars represent the standard error for each time point. Dose response curves for EcThrRS (**c**) and ObaO (**d**) were calculated from the data in a

and b by plotting the fractional velocity at each of seven different inhibitor concentrations against log [**1**]. Details of the fitting routines are presented in the Methods. CPM = counts per min.

however, the contrasting EcThrRS and ObaO profiles with the same **1** concentration ranges, clearly exclude that possibility in this case. Previous examples of partial inhibition mechanisms include the inhibition of reverse transcriptase by the non-nucleoside inhibitor tetrahydro-benzodiazepine[34] and inhibition of tyrosinase by substituted benzaldehydes.[35]

In the case of mupirocin, differences in resistant and susceptible IleRSs can be pinpointed to amino acid polymorphisms in the binding site, with resistance associated with eukaryotic-like enzymes.[36] For EcThrRS and ObaO all amino acid side chains that interact with tRNA, the catalytic Zn^{2+} ion and the Thr-AMP substrate intermediate in the *E. coli* enzyme are conserved (Supplementary Figure 2).[37] To investigate the origin of **1**-resistant ThrRS homologues we carried out a phylogenetic analysis of ObaO, homologues from other putative **1** BGCs, and primary copies of ThrRS from a range of organisms. Consistent with the conserved nature of this essential housekeeping protein we observed low bootstrap values at basal nodes of the tree, making it difficult to draw any firm conclusions about the origin of the **1** immunity gene. However, the resulting tree does suggest that the resistance isoforms are more closely related to one another than to housekeeping copies from the same species.

Conclusion

Using a combination of bioinformatics, mutational analyses, bioassays, and *in vitro* enzyme assays we identified the gene product ObaO as the immunity determinant of **1**, which functions as a resistant isoform of the **1** target ThrRS. Immunity guided natural product target discovery has been the subject of much interest in recent years,[18, 38] however there are still relatively few examples in which a hitherto unknown target has been identified *de novo* from its immunity determinant.[39, 40] Our data demonstrate the utility of this approach, especially in cases such as ours, when the inherent lability of the compound in aqueous solution precluded the generation of spontaneous mutants. We established that while expression of an extra copy of the native PfThrRS or the *E. coli* EcThrRS could restore some growth in the *obaO* deficient *P. fluorescens* strain, only complementation with ObaO restored WT-like growth and **1** production. We also

showed that expression of EcThRS and PfThrRS did not significantly alter the MIC for **1** in *E. coli* strains. These data indicate that ObaO does not provide immunity by a simple increase in levels of a functional ThrRS. In this preliminary study, the details of the specific mechanism of inhibition, and its competitive or non-competitive basis, have not been fully resolved. However, the data reported here do appear to rule out the simple model in which ObaO has acquired resistance to **1** owing to absence of inhibitor binding. Instead, the partial inhibition of ObaO by **1** suggests the possibility that **1** binds to a region of the active site that does not completely overlap with the site of threonine or ATP binding, but nevertheless influences the ability of ObaO to execute conformational changes associated with catalysis. Indeed, a similar mechanism for the ThrRS inhibitor borrelidin was proposed as part of the determination of the X-ray structure of the ThrRS:borrelidin complex.[26] One prediction of such a model is time dependent inhibitor behavior, which will be addressed in future experiments.

Our findings set the scene for future study on the mechanism by which **1** inhibits sensitive ThrRS, and into the resistance determinants of ObaO. In turn, this will enable rational drug design to generate improved versions of obafluorin.

METHODS

General Methods. All primers, plasmids and strains are reported in Supplementary Tables 2–3. All strains were maintained on lysogeny broth (LB) medium with appropriate selection at 37 °C for *E. coli* strains or 28 °C for *P. fluorescens* ATCC 39502 strains.

Construction of knockout, complementation and expression plasmids. Plasmids were constructed using standard ligation methods or using a Gibson Assembly® Cloning Kit (NEB) according to the manufacturer's instructions. Gene sequences were amplified from genomic DNA templates and vector backbones were prepared by either digestion with restriction endonucleases or PCR-amplification from plasmid DNA.

Δ*obaO* strains were generated using the suicide vector pTS1, constructed previously.[12] Primers were designed to amplify 800–1,200 bp flanking regions of the *obaO* protein coding sequence (PCS) for cloning into pTS1 between *Xba*I and *Avr*II sites, and *Avr*II and *Bmt*I sites. Flanking regions were designed to comprise 10–50 PCS codons at either end of the *obaO* gene to minimize polar effects, leaving a

truncated chromosomal copy of the gene with an in-frame deletion and internal *Avr*II site cloning artefact following double homologous recombination.

For genetic complementation, the *obaO*, *EcThrRS* and *PfThrRS* PCSs were cloned from start to stop either as *Bmt*I-*Kpn*I fragments (*obaO* and *EcThrRS*) or as a *Nde*I-*Xba*I fragment (*PfThrRS*). These were ligated into pJH10TS[12] for introduction and ectopic expression in the Δ*obaL*Δ*obaO* strain. The *obaO* and *EcThrRS* PCSs were also cloned into pET28a(+) as *Nde*I-*Xho*I fragments, for expression of N-terminally hexahistidine tagged proteins.

Mutagenesis and complementation experiments. pTS1-*obaO* knockout constructs were introduced into *P. fluorescens* ATCC 39502 strains via conjugation from *E. coli* S17-1 λpir and single-crossover mutants were selected for on LB supplemented with 50 μg mL^{-1} tetracycline (Tc^{50}). Positive colonies were cultured overnight in antibiotic-free medium to allow time for a second cross-over event to occur. *sacB* counter-selection could then be performed by plating culture dilutions on LB supplemented with 7% (w/v) sucrose to select against retention of the pTS1 vector backbone. Colony PCR was then performed to distinguish double cross-over mutants from WT colonies, with subsequent Sanger sequencing (Eurofins Genomics) to confirm the expected deletion.

For the WT strain, all of the resulting colonies tested retained the *obaO* gene, presumably due to selection against losing the **1** immunity gene. Consistent with this hypothesis, it was possible to delete *obaO* in the previously reported Δ*obaL* strain,[12] in which **1** biosynthesis is abolished. The resulting Δ*obaL*Δ*obaO* strain was subsequently complemented with pJH10TS-*obaO*, pJH10TS-*EcThrRS* and pJH10TS-*PfThrRS* constructs, or a pJH10TS empty vector control, via conjugation and positive clones were selected for on LB Tc^{50}. Clones were screened by colony PCR and confirmed by sequencing.

Analysis of growth and metabolite production. WT and recombinant *P. fluorescens* ATCC 39502 strains were grown in **1** Production Medium (OPM) comprising: yeast extract 0.5% (w/v), D-glucose 0.5% (w/v), $MgSO_4.7H_2O$ 0.01% (w/v), and $FeSO_4$ 0.01% (w/v), dissolved in Milli-Q (Merck Millipore) filtered water. A toothpick was used to inoculate 100 mL of OPM seed culture (250 mL Erlenmeyer flask) from a single colony, with subsequent growth for 24 h at 25 °C, 300 rpm. 1 mL of this culture was used to inoculate 100 mL (500 mL Erlenmeyer flask) OPM

production cultures, which were supplemented with either **2** in DMSO to a final concentration of 0.2 mM or DMSO only (final concentration of 0.2% DMSO in both cases).

For growth curves, production cultures were grown at 25 °C, 300 rpm and OD_{600} measurements relative to an OPM blank were recorded every hour for 10 h. For metabolite analysis, after 14 h of growth 1 mL of culture broth was extracted with an equal volume of ethyl acetate by mixing at 1,400 rpm for 15 min. Samples were then centrifuged (15,682 × *g* for 15 min), and the organic phase was collected and evaporated. The resulting extract was dissolved in MeCN (250 µL) and centrifuged (15,682 × *g* for 20 min) to remove any remaining cell debris, before HPLC analyses.

Analytical HPLC. Samples were analyzed on an Agilent 1100 system using a Gemini 3 µm NX-C18 110 Å, 150 x 4.6 mm column (Phenomenex) with a gradient elution: MeCN/0.1% (v/v) TFA (H_2O) gradient from 10/90 to 100/0 0–15 min, 100/0 for 15–16 min, gradient to 10/90 16–16.50 min and 10/90 for 16.50–23 min. The flow rate was 1 mL min^{-1} and the injection volume of each sample 10 µL. Chromatograms were recorded at 270 nm, the λ_{max} for **1**. The identity of **1** peaks were confirmed by comparison with an authentic standard. Retention times were: **1** 10.1 min, 4-nitrophenylethanol 7.7 min and 4-nitropenylacetate 7.9 min, the latter two compounds being shunt metabolites which are elevated in non-complemented Δ*obaL* strains.

Antibacterial assays. For agar diffusion bioassays, test strains were grown for 16-18 h in 5 mL LB cultures, containing appropriate selection. 500 µL of each culture was used to inoculate 50 mL LB cultures, which were incubated at 37 °C with 250 rpm until OD_{600} = 0.3–0.4. Cultures were diluted 1:10 with molten soft nutrient agar (SNA), before pouring into appropriately sized petri dishes to set. Serial dilutions of **1** were prepared in MeCN and 4 µL of each dilution was applied directly onto the SNA surface. Kanamycin (50 µg mL^{-1}) was used as a positive control, and MeCN as a negative control. Plates were incubated at 25 °C for 16–18 h. The MIC was defined as the lowest concentration of compound that resulted in a zone of inhibition. Experiments were carried out in at least triplicate for each strain.

Protein expression and purification. *E. coli* NiCo21(DE3) (NEB) carrying pLysS and either pET28a(+)-*EcThrRS* or pET28a(+)-*obaO* were used to express and purify proteins using immobilized metal affinity chromatography (IMAC) and size exclusion chromatography (SEC), as described previously.[12] Proteins were purified in a buffer

containing 25 mM Tris/HCl at pH 8.0 with NaCl (300 mM), $MgCl_2$ (10 mM) and glycerol (10% v/v), with the addition of 250 mM imidazole for IMAC elution Protein identities were confirmed by excising bands from SDS-PAGE gels, subjecting them to tryptic digest according to standard procedures adapted from Shevchenko et al.[41] and LCMS/MS analysis of peptide fragments with an Orbitrap-Fusion™ mass spectrometer (Thermo Fisher).

In vivo $tRNA^{Thr}$ transcription and purification. To obtain purified $tRNA^{Thr}$ for kinetics and aminoacylation assays, $tRNA^{Thr}$ was overexpressed in *E. coli* and purified by gel electrophoresis and electroelution as described in previous work.[42] *E. coli* $tRNA^{Thr}$ was expressed in BL21 *E. coli* cells and purified via phenol chloroform extraction. The $tRNA^{Thr}$ was then precipitated overnight in 2.5x volume EtOH and 0.1x volume sodium acetate and subjected to centrifugation. After washing the pellet with 75% v/v EtOH it was resuspended in 10 mM HEPES pH 6.0. This sample was then mixed with 6x blue loading dye and loaded into a large urea gel (6.5% polyacrylamide (19:1 acrylamide:bisacrylamide), 8 M urea, and 0.5 M sodium acetate pH 5.0). The gel was subject to 50 W until the dye front almost ran off the gel, at which point the gel was imaged via a UV light box and the $tRNA^{Thr}$ band was identified. This band was excised, chopped and placed into an electroeluter apparatus (Whatman/Schleicher & Schuell) overnight. After electroelution, the purified sample was again precipitated with 2.5x volume EtOH and 0.5x volume sodium acetate and then resuspended in TE pH 6.0 buffer.

Aminoacylation Assay. To measure the effects of **1** on ThrRS canonical tRNA charging activity, an assay modified from Ruan et al.[43] was used, where active enzyme was incubated with its necessary substrates and its activity measured usng ^{14}C labeled Thr and a liquid scintillation counter. Purified ThrRS protein (10 nM) was pre-incubated with varying concentrations of **1** for 10 min. After pre-incubation, ThrRS and **1** were added to a master reaction mixture with the final concentrations of 100 mM HEPES pH 7.0, 4 mM ATP, 10 mM $MgCl_2$, 50 μM ^{14}C labeled Thr (Moravek), and 5 μM $tRNA^{Thr}$. This mixture was then incubated for 10 min, with time points being taken at 1, 2.5, 5, and 10 min. At each time point, three 5 μL aliquots were spotted onto 5% (v/v) trichloroacetic acid (TCA) presoaked 3MM Whatman paper (Sigma-Aldrich). After letting the spots dry, the Whatman paper was washed three times with 5% TCA, and once with 95% v/v EtOH. Whatman paper was dried and the counts on each square

of paper analyzed with a liquid scintillation counter using Hydrofluor Liquid Scintillation Fluid (National Diagnostics). To calculate IC_{50}, fractional initial velocities (velocity of inhibited reaction/velocity in the absence of inhibitor) were plotted against the log of **1** concentration and then fitted to equation 1.[32]

$$\frac{v_i}{v_o} = \frac{1}{1 + \frac{[I]}{IC_{50}}} \quad (1)$$

For ObaO, a modified version of the equation was used to take into account the observed partial inhibition:

$$y = \frac{y_{max} - y_{min}}{1 + \frac{[I]}{IC_{50}}} y_{min} \quad (2)$$

Conflicts of interest

There are no conflicts to declare

Acknowledgements

This work was supported by the Biotechnology and Biological Sciences Research Council *via* institute strategic program BBS/E/J/00PR9791 (to the John Innes Centre (JIC), and research grant BB/P021506/1 to B.W. The contributions of P.W. and C.S.F. were supported by National Institute of General Medical Sciences grant GM54899-20. We thank L. Hill and G. Saalbach (JIC) for excellent metabolomics support.

Supporting Information Available: This material is available free of charge *via* the Internet. Figures S1-S3, Tables S1-S3, and Gene and Protein Sequences.

References

1. Bérdy, J. (2012) Thoughts and facts about antibiotics: Where we are now and where we are heading, *J. Antibiot. 65*, 385.

2. O'Neil, J. (2016) Tackling drug-resistant infections globally: final report and recommendations, *Review on Antimicrobial Resistance, UK Government and Wellcome Trust*.

3. Lowe, C., and Vederas, J. C. (1995) Naturally occurring β-lactones: Occurrence, syntheses and properties. A review, *Org. Prep. Proced. Int. 27*, 305-346.

4. Kluge, A. F., and Petter, R. C. (2010) Acylating drugs: redesigning natural covalent inhibitors, *Curr. Opin. Chem. Biol. 14*, 421-427.

5. Bachovchin, D. A., Ji, T., Li, W., Simon, G. M., Blankman, J. L., Adibekian, A., Hoover, H., Niessen, S., and Cravatt, B. F. (2010) Superfamily-wide portrait of serine hydrolase inhibition achieved by library-versus-library screening, *Proc. Natl. Acad. Sci. USA 107*, 20941-20946.

6. Potts, B. C., Albitar, M. X., Anderson, K. C., Baritaki, S., Berkers, C., Bonavida, B., Chandra, J., Chauhan, D., Cusack, J. C., Jr., Fenical, W., Ghobrial, I. M., Groll, M., Jensen, P. R., Lam, K. S., Lloyd, G. K., McBride, W., McConkey, D. J., Miller, C. P., Neuteboom, S. T. C., Oki, Y., Ovaa, H., Pajonk, F., Richardson, P. G., Roccaro, A. M., Sloss, C. M., Spear, M. A., Valashi, E., Younes, A., and Palladino, M. A. (2011) Marizomib, a proteasome inhibitor for all seasons: preclinical profile and a framework for clinical trials, *Curr. Cancer Drug Targets 11*, 254-284.

7. Weibel, E. K., Hadvary, P., Hochuli, E., Kupfer, E., and Lengsfeld, H. (1987) Lipstatin, an inhibitor of pancreatic lipase, produced by *Streptomyces toxytricini*. I. Producing organism, fermentation, isolation and biological activity, *J. Antibiot. 40*, 1081-1085.

8. Lehmann, J., Cheng, T.-Y., Aggarwal, A., Park, A. S., Zeiler, E., Raju, R. M., Akopian, T., Kandror, O., Sacchettini, J. C., Moody, D. B., Rubin, E. J., and Sieber, S. A. (2018) An antibacterial β-Lactone kills *Mycobacterium tuberculosis* by disrupting mycolic acid biosynthesis, *Angew. Chem. Int. Ed. 57*, 348-353.

9. Gersch, M., Gut, F., Korotkov, V. S., Lehmann, J., Böttcher, T., Rusch, M., Hedberg, C., Waldmann, H., Klebe, G., and Sieber, S. A. (2013) The mechanism of caseinolytic protease (ClpP) inhibition, *Angew. Chem. Int. Ed. 52*, 3009-3014.

10. Vitale, R., Ottonello, G., Petracca, R., Bertozzi, S. M., Ponzano, S., Armirotti, A., Berteotti, A., Dionisi, M., Cavalli, A., Piomelli, D., Bandiera, T., and Bertozzi, F. (2014) Synthesis, structure–activity, and structure–stability relationships of 2-substituted-*N*-(4-oxo-3-oxetanyl) *N*-acylethanolamine acid amidase (NAAA) inhibitors, *ChemMedChem 9*, 323-336.

11. Robinson, S. L., Christenson, J. K., and Wackett, L. P. (2019) Biosynthesis and chemical diversity of β-lactone natural products, *Nat. Prod. Rep. 36*, 458-475.

12. Scott, T. A., Heine, D., Qin, Z., and Wilkinson, B. (2017) An L-threonine transaldolase is required for L-threo-β-hydroxy-α-amino acid assembly during obafluorin biosynthesis, *Nat. Commun. 8*, 15935.

13. Schaffer, J. E., Reck, M. R., Prasad, N. K., and Wencewicz, T. A. (2017) β-Lactone formation during product release from a nonribosomal peptide synthetase, *Nat. Chem. Biol. 13*, 737.

14. Wells, J. S., Trejo, W. H., Principe, P. A., and Sykes, R. B. (1984) Obafluorin, a novel β-lactone produced by *Pseudomonas fluorescens*. Taxonomy, fermentation and biological properties, *J. Antibiot. 37*, 802-803.

15. Tymiak, A. A., Culver, C. A., Malley, M. F., and Gougoutas, J. Z. (1985) Structure of obafluorin: an antibacterial β-lactone from *Pseudomonas fluorescens*, *J. Org. Chem. 50*, 5491-5495.

16. Cundliffe, E., and Demain, A. L. (2010) Avoidance of suicide in antibiotic-producing microbes, *J. Ind. Microbiol. Biotechnol. 37*, 643-672.

17. Thaker, M. N., Wang, W., Spanogiannopoulos, P., Waglechner, N., King, A. M., Medina, R., and Wright, G. D. (2013) Identifying producers of antibacterial compounds by screening for antibiotic resistance, *Nat. Biotechnol. 31*, 922-927.

18. Alanjary, M., Kronmiller, B., Adamek, M., Blin, K., Weber, T., Huson, D., Philmus, B., and Ziemert, N. (2017) The Antibiotic Resistant Target Seeker (ARTS), an exploration engine for antibiotic cluster prioritization and novel drug target discovery, *Nucleic Acids Res. 45*, W42-W48.

19. Panter, F., Krug, D., Baumann, S., and Müller, R. (2018) Self-resistance guided genome mining uncovers new topoisomerase inhibitors from myxobacteria, *Chem. Sci. 9*, 4898-4908.

20. Ibba, M., and Söll, D. (2000) Aminoacyl-tRNA Synthesis, *Annu. Rev. Biochem. 69*, 617-650.

21. Cochrane, R. V. K., Norquay, A. K., and Vederas, J. C. (2016) Natural products and their derivatives as tRNA synthetase inhibitors and antimicrobial agents, *MedChemComm 7*, 1535-1545.

22. Francklyn, C. S., and Mullen, P. (2019) Progress and challenges in aminoacyl-tRNA synthetase-based therapeutics, *J. Biol. Chem. 294*, 5365–5385.

23. Reader, J. S., Ordoukhanian, P. T., Kim, J. G., de Crecy-Lagard, V., Hwang, I., Farrand, S., and Schimmel, P. (2005) Major biocontrol of plant tumors targets tRNA synthetase, *Science 309*, 1533.

24. Hughes, J., and Mellows, G. (1978) Inhibition of isoleucyl-transfer ribonucleic acid synthetase in *Escherichia coli* by pseudomonic acid, *Biochem. J. 176*, 305-318.

25. Poralla, K., and Zahner, H. (1968) Metabolic products of microorganisms. 62. The inhibition of the incorporation of threonine in sRNA in cell-free systems and of the synthesis of proteins and nucleic acids in the cell by the antibiotic borrelidin, *Arch. Mikrobiol. 61*, 143-153.

26. Fang, P., Yu, X., Jeong, S. J., Mirando, A., Chen, K., Chen, X., Kim, S., Francklyn, C. S., and Guo, M. (2015) Structural basis for full-spectrum inhibition of translational functions on a tRNA synthetase, *Nat. Commun. 6*, 6402.

27. El-Sayed, A. K., Hothersall, J., Cooper, S. M., Stephens, E., Simpson, T. J., and Thomas, C. M. (2003) Characterization of the mupirocin biosynthesis gene cluster from *Pseudomonas fluorescens* NCIMB 10586, *Chem. Biol. 10*, 419-430.

28. Olano, C., Moss, S. J., Braña, A. F., Sheridan, R. M., Math, V., Weston, A. J., Méndez, C., Leadlay, P. F., Wilkinson, B., and Salas, J. A. (2004) Biosynthesis of the angiogenesis inhibitor borrelidin by *Streptomyces parvulus* Tü4055: insights into nitrile formation, *Mol. Microbiol. 52*, 1745-1756.

29. Du, Y.-L., Alkhalaf, L. M., and Ryan, K. S. (2015) In vitro reconstitution of indolmycin biosynthesis reveals the molecular basis of oxazolinone assembly, *Proc. Natl. Acad. Sci. USA 112*, 2717-2722.

30. Eggert, U. S., Ruiz, N., Falcone, B. V., Branstrom, A. A., Goldman, R. C., Silhavy, T. J., and Kahne, D. (2001) Genetic basis for activity differences between vancomycin and glycolipid derivatives of vancomycin, *Science 294*, 361-364.

31. Pu, Y., Lowe, C., Sailer, M., and Vederas, J. C. (1994) Synthesis, stability, and antimicrobial activity of (+)-obafluorin and related β-lactone antibiotics, *J. Org. Chem. 59*, 3642-3655.

32. Connolly, J. A., Wilson, A., Macioszek, M., Song, Z., Wang, L., Mohammad, H. H., Yadav, M., di Martino, M., Miller, C. E., Hothersall, J., Haines, A. S., Stephens, E. R., Crump, M. P., Willis, C. L., Simpson, T. J., Winn, P. J., and Thomas, C. M. (2019) Defining the genes for the final steps in biosynthesis of the complex polyketide antibiotic mupirocin by *Pseudomonas fluorescens* NCIMB10586, *Sci. Rep. 9*, 1542.

33. Copeland, R. A. (2004) In *Enzymes: A Practical Introduction to Structure, Mechanism, and Data Analysis* 2nd ed., pp 270-287, John Wiley & Sons.

34. Spence, R. A., Kati, W. M., Anderson, K. S., and Johnson, K. A. (1995) Mechanism of inhibition of HIV-1 reverse transcriptase by nonnucleoside inhibitors, *Science 267*, 988-993.

35. Nihei, K.-I., and Kubo, I. (2017) Substituent effect of benzaldehydes on tyrosinase inhibition, *Plant Physiol. Biochem. 112*, 278-282.

36. Nakama, T., Nureki, O., and Yokoyama, S. (2001) Structural basis for the recognition of isoleucyl-adenylate and an antibiotic, mupirocin, by isoleucyl-tRNA synthetase, *J. Biol. Chem. 276*, 47387-47393.

37. Sankaranarayanan, R., Dock-Bregeon, A.-C., Romby, P., Caillet, J., Springer, M., Rees, B., Ehresmann, C., Ehresmann, B., and Moras, D. (1999) The structure of threonyl-tRNA synthetase-tRNA^{Thr} complex enlightens its repressor activity and reveals an essential zinc ion in the active site, *Cell 97*, 371-381.

38. Almabruk, K. H., Dinh, L. K., and Philmus, B. (2018) Self-resistance of natural product producers: past, present, and future focusing on self-resistant protein variants, *ACS Chem. Biol. 13*, 1426-1437.

39. Kling, A., Lukat, P., Almeida, D. V., Bauer, A., Fontaine, E., Sordello, S., Zaburannyi, N., Herrmann, J., Wenzel, S. C., König, C., Ammerman, N. C., Barrio, M. B., Borchers, K., Bordon-Pallier, F., Brönstrup, M., Courtemanche, G., Gerlitz, M., Geslin, M., Hammann, P., Heinz, D. W., Hoffmann, H., Klieber, S., Kohlmann, M., Kurz, M., Lair, C., Matter, H., Nuermberger, E., Tyagi, S., Fraisse, L., Grosset, J. H., Lagrange, S., and Müller, R. (2015) Targeting DnaN for tuberculosis therapy using novel griselimycins, *Science 348*, 1106-1112.

40. Baumann, S., Herrmann, J., Raju, R., Steinmetz, H., Mohr, K. I., Hüttel, S., Harmrolfs, K., Stadler, M., and Müller, R. (2014) Cystobactamids: Myxobacterial Topoisomerase Inhibitors Exhibiting Potent Antibacterial Activity, *Angew. Chem. Int. Ed. 53*, 14605-14609.

41. Shevchenko, A., Wilm, M., Vorm, O., and Mann, M. (1996) Mass spectrometric sequencing of proteins from silver-stained polyacrylamide gels, *Anal. Chem. 68*, 850-858.

42. Francklyn, C. S., First, E. A., Perona, J. J., and Hou, Y.-M. (2008) Methods for kinetic and thermodynamic analysis of aminoacyl-tRNA synthetases, *Methods 44*, 100-118.

43. Ruan, B., Bovee, M. L., Sacher, M., Stathopoulos, C., Poralla, K., Francklyn, C. S., and Söll, D. (2005) A unique hydrophobic cluster near the active site contributes to differences in borrelidin inhibition among threonyl-tRNA synthetases, *J. Biol. Chem. 280*, 571-577.

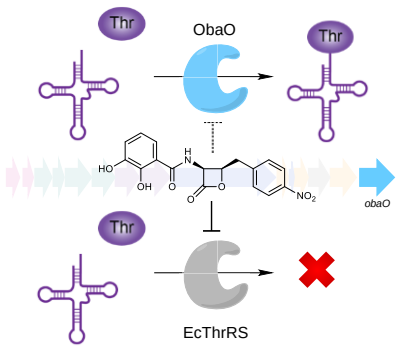
Thr
ObaO
Thr
HO
OH
H
N
O
O
O
NO2
obaO
Thr
EcThrRS